



## Computational selection of inhibitors of A $\beta$ aggregation and neuronal toxicity

Deliang Chen<sup>a,†</sup>, Zane S. Martin<sup>b,†</sup>, Claudio Soto<sup>b,d,\*</sup>, Catherine H. Schein<sup>a,c,\*</sup>

<sup>a</sup> Sealy Center for Structural Biology and Molecular Biophysics, Department of Biochemistry and Molecular Biology, UTMB, Galveston, TX 77555-0857, USA

<sup>b</sup> George and Cynthia Mitchell Center for Neurodegenerative diseases, Department of Neurology, Neurosciences and Cell Biology UTMB, Galveston, TX 77555-1045, USA

<sup>c</sup> Department of Microbiology and Immunology, and Sealy Center for Vaccine Development, UTMB, Galveston, TX 77555-0857, USA

<sup>d</sup> Department of Neurology, University of Texas Medical School at Houston, Houston, TX 77030, USA

### ARTICLE INFO

#### Article history:

Received 27 February 2009

Revised 13 May 2009

Accepted 18 May 2009

Available online 27 May 2009

#### Keywords:

Alzheimer's disease

Amyloid fibrils

Aggregation inhibitors

Pharmacophore modeling

Database screening

Aggregation reversing

### ABSTRACT

Alzheimer's disease (AD) is characterized by the cerebral accumulation of misfolded and aggregated amyloid- $\beta$  protein (A $\beta$ ). Disease symptoms can be alleviated, in vitro and in vivo, by ' $\beta$ -sheet breaker' pentapeptides that reduce plaque load. However the peptide nature of these compounds, made them biologically unstable and unable to penetrate membranes with high efficiency. The main goal of this study was to use computational methods to identify small molecule mimetics with better drug-like properties. For this purpose, the docked conformations of the active peptides were used to identify compounds with similar activities. A series of related  $\beta$ -sheet breaker peptides were docked to solid state NMR structures of a fibrillar form of A $\beta$ . The lowest energy conformations of the active peptides were used to design three dimensional (3D)-pharmacophores, suitable for screening the NCI database with Unity. Small molecular weight compounds with physicochemical features and a conformation similar to the active peptides were selected, ranked by docking and biochemical parameters. Of 16 diverse compounds selected for experimental screening, 2 prevented and reversed A $\beta$  aggregation at 2–3  $\mu$ M concentration, as measured by Thioflavin T (ThT) fluorescence and ELISA assays. They also prevented the toxic effects of aggregated A $\beta$  on neuroblastoma cells. Their low molecular weight and aqueous solubility makes them promising lead compounds for treating AD.

© 2009 Elsevier Ltd. All rights reserved.

### 1. Introduction

Alzheimer's disease (AD) is the most common form of dementia in the elderly, affecting 6–10% of people over the age of 65.<sup>1</sup> A progressive neurodegenerative disease,<sup>2</sup> AD's clinical symptoms include personality and behavioral changes, periods of disorientation, difficulty communicating, and gradual loss of memory. Although the molecular basis of AD has been extensively studied, there is still no early diagnosis or cure. The hallmark neuropathological features of the disease are the accumulation of extracellular plaques composed of the amyloid- $\beta$  protein (A $\beta$ ), and intracellular, hyper-phosphorylated tau forming neurofibrillary tangles and dystrophic neurites. The progression of A $\beta$  plaque deposition in humans begins in the temporal cortex, proceeds to the hippocampus and then to the entorhinal and transentorhinal cortices,<sup>3</sup> while tau deposits progress in the opposite direction.<sup>4</sup> Several possible molecular mechanisms may initiate AD. However, considerable genetic and biochemical evidence suggests that A $\beta$  misfolding,

oligomerization and accumulation in the brain is the primary cause of the neuronal dysfunction.<sup>5</sup>

Amyloid is a generic term used to refer to protein aggregates adopting a cross- $\beta$ -sheet structure.<sup>6</sup> Several studies have shown that the aggregation and fibril formation of A $\beta$  involves a change in conformation, from a (soluble) helical or coiled structure to an insoluble oligomer.<sup>7</sup> Solid state NMR studies of 6–10 nm in diameter fibrils of purified A $\beta$  have revealed an underlying superstructure of anti-parallel intra-molecular  $\beta$ -strands stabilized predominantly by backbone hydrogen bonds and salt bridges, and parallel, inter-molecular  $\beta$ -sheets stabilized predominantly by backbone hydrogen bonds and hydrophobic interactions.<sup>8–11</sup> A network of inter- and intra-molecular hydrogen bonds maintains the stability of the fibril once it has formed.<sup>12–15</sup> A $\beta$  can form amyloid-like fibrils in the absence of other proteins,<sup>7</sup> indicating that the potential to form amyloid originates within its own sequence. Substitution of hydrophilic for hydrophobic residues in the central hydrophobic region of A $\beta$  (17–21) impairs fibril formation,<sup>12,16–21</sup> and peptides designed to mimic the structure of this region could inhibit aggregation. A series of ' $\beta$ -sheet breaker peptides' were designed based on A $\beta$  amino acids 17–20 (LVFF), and then chemically modified to obtain more active and stable pentapeptides with the basic sequence LPFFD.<sup>22–25</sup> Such compounds were demonstrated by us and other groups to

\* Corresponding authors. Tel.: +1 713 500 7086; fax: +1 713 500 0667 (C.S.); tel.: +1 409 747 6843; fax: +1 409 747 6000 (C.H.S.).

E-mail addresses: [claudio.soto@uth.tmc.edu](mailto:claudio.soto@uth.tmc.edu) (C. Soto), [chschein@utmb.edu](mailto:chschein@utmb.edu), [dechen@utmb.edu](mailto:dechen@utmb.edu) (C.H. Schein).

<sup>†</sup> The first two authors contributed equally to this study.

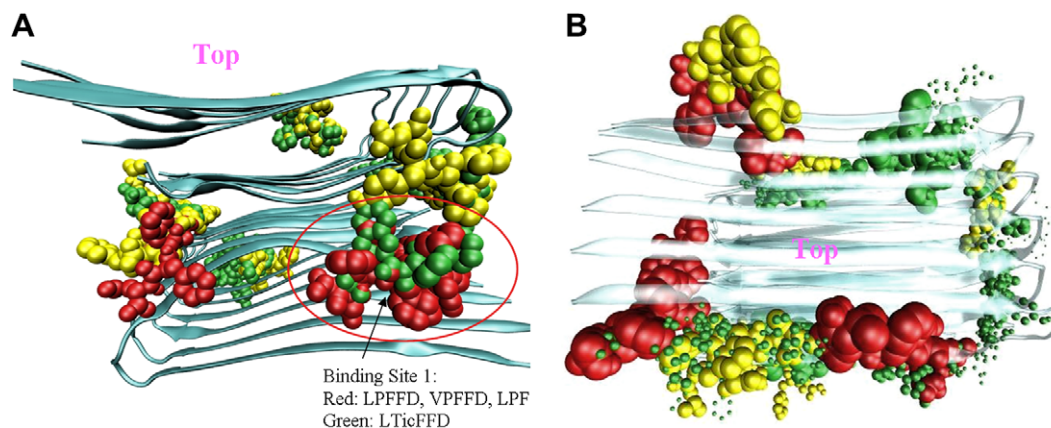


**Figure 1.** Docking positions of 30  $\beta$ -sheet breaker pentapeptides on two fibril structures of A $\beta$ , A $\beta$ 40m2\_1.pdb (left), and A $\beta$ 40p2\_1.pdb (right), colored according to their activities in preventing A $\beta$  aggregation (red, highest relative activities >70% of LPFFD activity, or  $\ln(\text{Act}) > 4.25$ ; green, lowest relative activities  $\leq 7\%$  or  $\ln(\text{Act}) < 2.0$ ; yellow have intermediate activities ( $70 > \text{Relative activity} > 8$ ; or  $4.25 > \ln(\text{Act}) > 2$ ). The top of the fibril is indicated for orientation purposes.

be active in destabilizing the pathological A $\beta$  conformation, leading to both inhibition of amyloid formation and disassembly of pre-formed fibrils. The lead  $\beta$ -sheet breaker peptide is able to inhibit and disassemble amyloid fibrils in vitro, to prevent A $\beta$  neurotoxicity in cell culture, and to arrest and dissolve amyloid plaques in several in vivo animals models.<sup>23,24,26</sup> Treatment with this peptide also inhibited neuronal death, brain inflammation and memory impairment in vivo.<sup>23,24</sup> In addition, the modified peptide showed low toxicity, low immunogenicity, high solubility and reasonably high brain uptake.<sup>23,25</sup> In spite of the good activity in vivo, the major weaknesses of this peptide are that it is rapidly degradable and has low permeability to cross biological barriers.<sup>25</sup> These are serious limitations because a more frequent administration of large quantities by inconvenient routes (injection) is likely to be necessary. It may also be difficult or impossible to reach the appropriate doses for anti-amyloid activity in the large volume of the human brain.

The major goal of the current study is to use the knowledge accumulated over several years on the structure–activity relationship studies of  $\beta$ -sheet breaker peptides and their 3-dimensional structure to design and identify small molecule peptidomimetic compounds. For this purpose, we used a computational/docking approach to identify features of this peptide series that correlated with their ability to prevent A $\beta$  aggregation. We docked the peptide series to the fibrillar structures of A $\beta$  determined from solid state NMR data. While the docking energies could not be used to discriminate the best inhibitors of aggregation, active peptides preferentially bound to different sites on the fibril from those favored by inactive ones. We used the docked conformations of the peptides to obtain a 3D-molecular pharmacophore, which could be used with the UNITY program to screen the NIH library for compounds with the desired physicochemical properties. These were initially ranked based on the number of pharmacophores they matched and then by molecular docking to the experimentally determined structures of fibrillar A $\beta$ . The compounds with the best docking scores at the optimal peptide positions were further selected for solubility (low log *P*: the coefficient for solvent partitioning between 1-octanol and water), and low molecular weight. Finally, 16 compounds from the NCI library<sup>27</sup> (<http://dtp.nci.nih.gov/webdata.html>) were selected and assayed for their ability to inhibit and reverse the aggregation of A $\beta$ , in three different assays, and the toxic effects of aggregates on neuronal cells. Two compounds inhibited A $\beta$  aggregation and cytotoxicity to neuroblastoma cells. They are thus promising lead compounds for developing novel treatments for AD.

## 2. Results

### 2.1. Docking of $\beta$ -sheet breaker peptides and selected compounds to the A $\beta$ fibril

We first docked  $\beta$ -sheet breaker peptides to the fibril structures, to relate binding energies to their activities in disaggregating A $\beta$ . Thirty pentapeptides, with known and varying ability to inhibit A $\beta$  aggregation, were initially docked to the larger grid box (see Sections 5.2 and 5.3), to find the site on the fibril for which they had the highest affinity. While the peptides all had similar AUTODOCK scores (Table S1, Supplementary), their preferred docking sites were quite different (Fig. 1). The most active peptides (red; peptides with relative activities >70 in Supplementary data Table 1s) bound to a few sites on each fibril structure, while the inactive ones showed less specificity. The first preferred docking site includes residues GLU11-PHE19 and LEU34-VAL40 of 4 outer neighbor monomers. The second preferred docking site includes residues 37–39 from the upper 6 monomers and residues 28–32 from the bottom 6 monomers.

For pharmacophore design and compound docking, two optimal binding sites (Fig. 2) were selected for each fibril model. The first binding sites, where LPFFD has the best AUTODOCK score to the A $\beta$  fibril models A $\beta$ 40m2\_1.pdb and A $\beta$ 40p2\_1.pdb, are the same as the preferred docking sites shown in Figure 1. The second binding site chosen is that with the next lowest docking energy that is at least 15 Å away from the first site. The second binding sites for both fibril structures, A $\beta$ 40m2\_1.pdb and A $\beta$ 40p2\_1.pdb, are close to the docking site of DFPPL to A $\beta$  identified by NMR,<sup>28</sup> which primarily interacted with residues Lys16-Phe20 on the top surface of several monomers. The most active  $\beta$ -sheet breaker pentapeptides<sup>25</sup> bind around site 1 in both structures. For comparison purposes, all 30 peptides were also docked to two binding sites on the A $\beta$ 40m2\_1.pdb and A $\beta$ 40p2\_10.pdb models (Fig. 2). These sites were also later used to determine the docking energy of compounds selected from NCI database (to match the pharmacophores). Based on the docking results, active compounds, including the lead compound LPFFD which is used for pharmacophore design, can form hydrogen bonds with the backbone hydrogen bond forming atoms. We will discuss the preferred interactions between the active compounds and the fibril later.

### 2.2. Pharmacophore design

We assumed that the preferred docking sites for the active peptides represented optimal binding positions on the A $\beta$  fibril. The

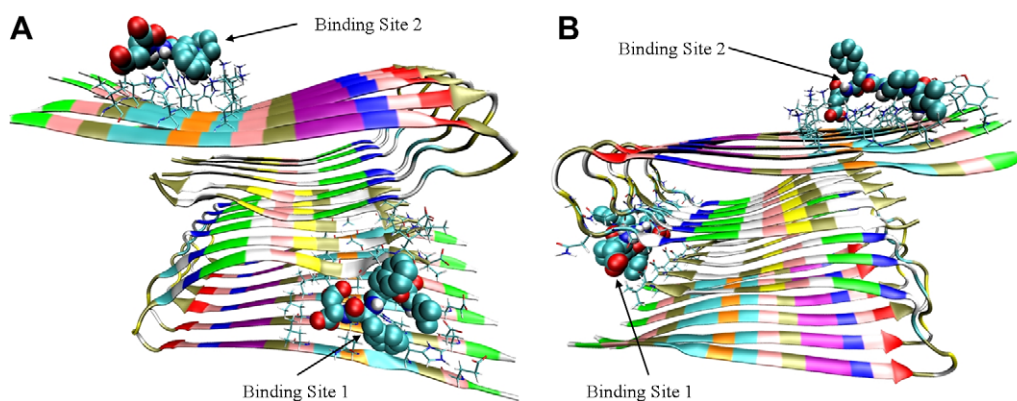


**Figure 2.** (A, B) Preferred docking sites for LPFFD (shown with CPK coloring) to the fibril structures (A) A $\beta$ 40m2\_1.pdb and (B) A $\beta$ 40p2\_1.pdb.

pattern of bonds formed by LPFFD with the fibril in the lowest energy docked conformation were analyzed, to derive features and distance constraints for the design of four 3D-pharmacophores, based on docking to A $\beta$ 40m2\_1.pdb and A $\beta$ 40p2\_1.pdb at sites 1 and 2 (Fig. 3).

### 2.3. Database screening with UNITY

The pharmacophores were used with the UNITY program to search ~250,000 structures from the NCI library. The numbers of compounds that match each of the four 3D-pharmacophores were 980, 1130, 1720 and 1440 for pharmacophore 1, 2, 3 and 4, respectively. These were docked to the A $\beta$  fibril structures at sites 1 and 2. The number of compounds with lower docking energies than LPFFD was 68, 26, 61 and 33 for site 1 of A $\beta$ 40m2\_1.pdb, site 2 of A $\beta$ 40m2\_1.pdb, site 1 of A $\beta$ 40p2\_1.pdb and site 2 of A $\beta$ 40p2\_1.pdb, respectively. We further reduced the number of compounds for assay by giving highest priority to compounds selected by UNITY as a potential match for multiple pharmacophores (27 compounds were identified as similar to all 4 pharmacophores, 42 were found in 3 of the 4, 105 in 2, and the remaining 4800 compounds matched only one pharmacophore).

We chose 31 compounds with higher calculated docking affinities than LPFFD from the 69 compounds that matched at least 3 pharmacophores. Although we knew from the peptide series that docking energies alone are not sufficient to distinguish the active peptides from the inactive ones, it was also clear that to reverse the aggregation, an inhibitor should preferentially bind A $\beta$ . Of these, 16 were selected based on their physical properties (log *P* not over 5, molecular weight not over 500, number of hydrogen

bond acceptors (HBA) not over 10, and hydrogen bond donors (HBD) not over 5). If two or more parameters were out of range, the compounds would not be selected. The structure of the 16 compounds and their NCI number are shown in Figure 4. Table 1 lists their docking scores and physicochemical properties.

### 2.4. Bioassays

The selected molecules were first screened using a medium throughput in vitro assay based on the specific interaction between amyloid fibrils and ThT. Incubation of soluble A $\beta$  alone for 24 h resulted in extensive formation of amyloid fibrils (Fig. 5). However, co-incubation with an equimolar concentration of several of the compounds led to a highly significant inhibition of fibril formation. Two compounds, termed BSBM6 and BSBM7 ( $\beta$ -sheet breaker mimetic 6 and 7, respectively, Fig. 5A), were selected for further studies, since they showed the highest reproducible inhibition in all assays. Equimolar concentration of these compounds led to >70% inhibition of fibril formation (Fig. 5B). In contrast, an inactive compound (C1 from the initial series) did not alter A $\beta$  amyloidogenesis at the concentration studied. BSBM 6 and 7 were also able to disassemble pre-formed A $\beta$  fibrils (Fig. 5C), decreasing the amount of pre-formed fibrils by >70%. Again, C1 did not alter significantly the amount of fibrils. As controls the compounds alone were added to the ThT assay and the results showed that none of the compounds studied altered ThT fluorescence (data not shown). To confirm the results using an in vitro assay based on a different principle, and to assess the concentration-dependent effect of the compounds in A $\beta$  aggregation, we measured the compounds' activity using a sedi-

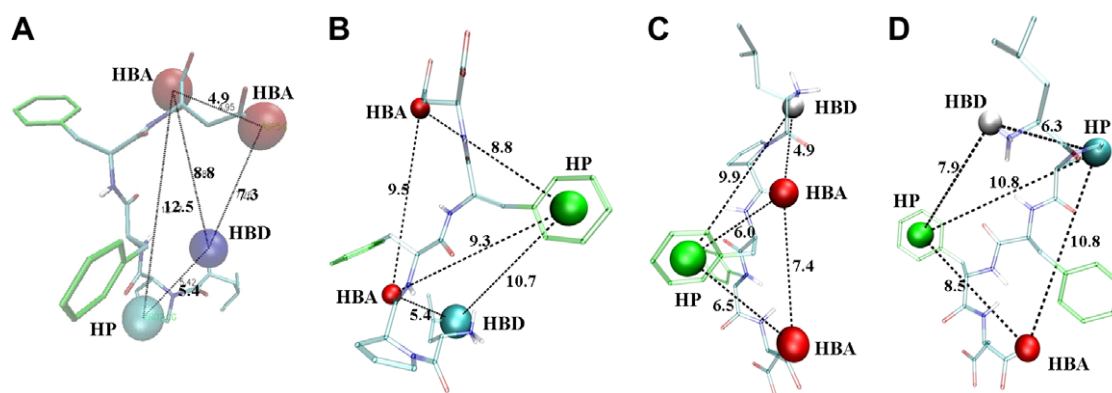


**Figure 3.** Pharmacophores designed based on the docking model of LPFFD to (A, B) docking sites 1, 2 of the fibril structure A $\beta$ 40m2\_1. (C, D) Docking sites 1, 2 of the fibril structure A $\beta$ 40p2\_1.

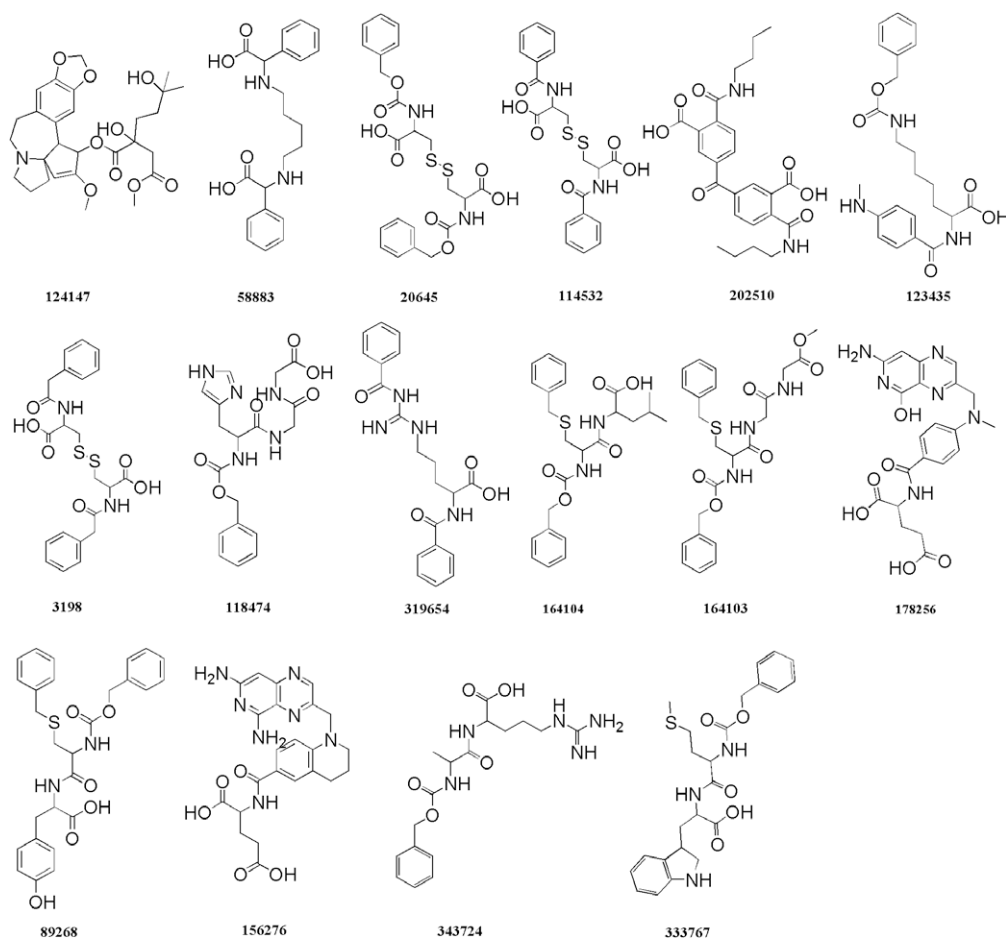


**Figure 4.** Structures and NCI number of NCI compounds selected for bioassays.

mentation assay, and measured the amount of A $\beta$  using ELISA. Increasing concentrations of BSBM6 or BSBM7 inhibited aggregation, reaching a maximum of around 80% at approximately

around equimolarity with the A $\beta$  concentration (4  $\mu$ M; Fig. 5D). The IC<sub>50</sub> values for BSBM6 and BSBM7 in this assay are 2.75 and 1.95  $\mu$ M, respectively.

**Table 1**

AUTODOCK scores ('binding energy') and physical properties of compounds selected for bioassays. The most active compounds are bold, the least active (control in Fig. 4) is underlined

Compound	NCI number	AUTODOCK Score at each binding site (binding energy kcal/mol)				Num. of pharm. matched	Num. of HBD	Num. of HBA	cLog P
		BS1 <sup>a</sup> of Model 1 <sup>c</sup>	BS2 <sup>b</sup> of Model 1 <sup>c</sup>	BS1 <sup>a</sup> of Model 2 <sup>d</sup>	BS2 <sup>b</sup> of Model 2 <sup>d</sup>				
<b>1</b>	<b>NSC124147</b>	<b>-16.2</b>	<b>-16.3</b>	<b>-15.4</b>	<b>-14.1</b>	<b>3</b>	<b>2</b>	<b>10</b>	<b>2.05</b>
<b>2</b>	NSC58883	-11.8	-9.6	-12.4	-9.9	3	4	6	-0.05
<b>3</b>	NSC20645	-10.7	-11.6	-9.4	-8.5	4	4	8	2.29
<b>4</b>	NSC114532	-10.9	-11.1	-9.6	-8.9	4	4	6	1.37
<b>5</b>	NSC202510	-11.4	-11.3	-13.5	-11.6	3	4	7	3.59
<b>6</b>	<b>NSC123435</b>	<b>-11.8</b>	<b>-12.1</b>	<b>-11.8</b>	<b>-11.6</b>	<b>4</b>	<b>4</b>	<b>6</b>	<b>2.81</b>
<b>7</b>	<b>NSC3198</b>	<b>-12.1</b>	<b>-11.3</b>	<b>-10.5</b>	<b>-11.0</b>	<b>4</b>	<b>4</b>	<b>6</b>	<b>1.83</b>
<b>8</b>	NSC118474	-10.6	-11.2	-11.1	-10.9	4	5	8	-0.83
<b>9</b>	NSC319654	-11.9	-11.6	-11.7	-12.3	4	5	6	1.7
<b>10</b>	NSC164104	-11.2	-11.9	-10.1	-9.5	4	3	5	3.84
<b>11</b>	NSC164103	-10.9	-11.9	-9.8	-9.6	4	3	6	1.56
<b>12</b>	NSC178256	-10.7	-8.7	-12.3	-11.8	3	5	10	0.6
<b>13</b>	NSC89268	-11.7	-12.6	-9.7	-8.8	3	4	6	3.67
<b>14</b>	NSC156276	-11.8	-10.8	-16.3	-12.7	3	5	12	-0.35
<b>15</b>	NSC343724	-10.7	-9.2	-11.5	-10.5	3	6	8	-0.37
<b>16</b>	NSC333767	-11.5	-12.3	-9.7	-8.6	4	4	6	2.99
DPFFL		-10.6	-8.8	-10.2	-11.5				
LPFFD		-10.1	-9.0	-11.7	-10.8				

<sup>a</sup> Binding site 1.

<sup>b</sup> Binding site 2.

<sup>c</sup> The fibril structures A $\beta$ 40m2\_1.pdb.

<sup>d</sup> The fibril structures A $\beta$ 40p2\_1.pdb.



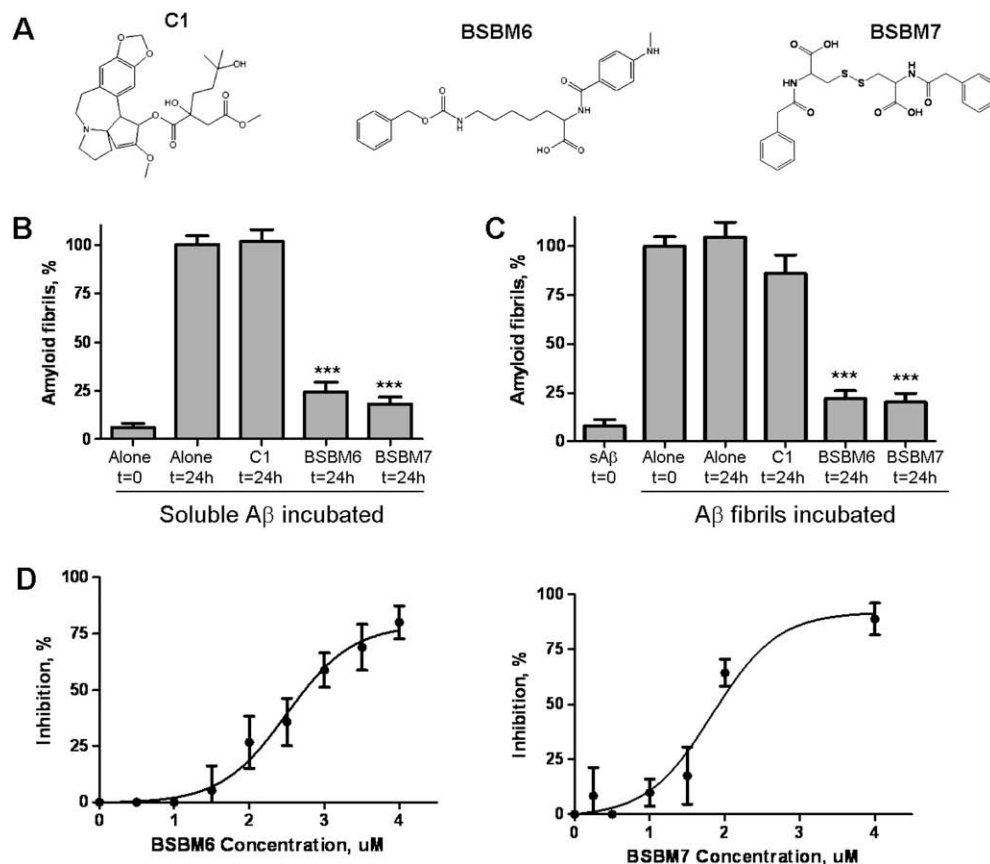


**Figure 5.** In vitro activity of selected compounds on Aβ fibrillogenesis. (A) Chemical structure of two putative β-sheet breaker mimetics: β-sheet breaker mimetic 6 (BSBM6) and β-sheet breaker mimetic 7 (BSBM7), and the inactive C1 control compound. (B) The effect of selected compounds on Aβ amyloid formation was studied by incubation of soluble Aβ1–42 in the absence or the presence of an equimolar concentration of the molecules. Amyloid formation was measured by ThT, as described in Methods. Results are expressed as a percentage of fibrils formed by the peptide incubated alone for 24 h. The data was analyzed by student-*t* test by comparing each result with the control of Aβ incubated alone. \*\*\*, *P* < 0.001. (C) The ability of the compounds to disassemble pre-form fibrils was assessed by incubation of the molecules with Aβ aggregates made by pre-incubation of Aβ1–42 alone. The amount of fibrils before and after incubation with the compounds was studied by ThT. Results are expressed as a percentage of fibrils remaining after incubation alone for 24 h. The data was analyzed by student-*t* test by comparing with the control of fibrils incubated alone. \*\*\*, *P* < 0.001. (D) The concentration-dependent effect of BSBM6 and BSBM7 on Aβ aggregation was studied by incubating soluble Aβ1–42 with various quantities of the compounds for 24 h at 37 °C. Formation of aggregates was quantified by sedimentation assay, followed by ELISA, as described in Methods. The data in panels B, C and D corresponds to the average ± standard error of three different experiments.

### 2.5. BSBM6 and 7 reduce the neurotoxicity of Aβ aggregates

Aβ aggregates decrease the viability of cultured N2A mouse neuroblastoma cells (Fig. 6). Treatment with Aβ pre-incubated for 24 h, which contain a mixture of oligomeric and fibrillar species, substantially reduced cell viability. This effect could be prevented if Aβ was incubated with equimolar concentrations of BSBM6 and 7, indicating that formation of toxic forms of misfolded Aβ was substantially inhibited. The control compound 1 did not prevent Aβ cytotoxicity and indeed, may have increased cell death. None of the compounds tested, on their own, were significantly toxic to cells (as measured by the MTS assay) even at quantities 10 times higher than the active concentration (data not shown).

### 3. Discussion

There have been extensive studies of the mechanism of Aβ misfolding and aggregation,<sup>20,29,30</sup> and many different compounds have been identified that interfere with this pathway (for reviews, see<sup>31–35</sup>). We previously reported that Aβ fibrillogenesis can be prevented and reversed by short peptides designed to bind and inhibit β-sheet misfolding of Aβ (β-sheet breaker peptides). These peptides are active in vitro, in cells and in several in vivo animal models of AD.<sup>22–26</sup> Moreover, they are well-tolerated in humans,

although they exhibited a short half-life and are not orally bioavailable.<sup>25</sup> Using the knowledge gained about the structure–activity

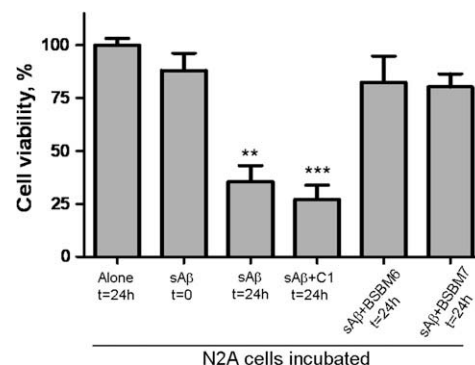


**Figure 6.** The activity of selected compounds on preventing Aβ neurotoxicity was studied in cell cultures. N2A cells were treated with soluble Aβ1–42 (3.3 μM) which was pre-incubated for 48 h either alone or in the presence of 3.3 μM of BSBM6, BSBM7 or C1. After 24 h incubation with the mixture peptide/compounds, cell viability was evaluated by the MTS assay. Data represent the average ± standard error of 3 determinations and is expressed as the percentage of viability obtained when cells were incubated alone for 24 h. Data for the compounds was statistically compared with cells incubated alone using the student-*t* test. \*\**P* < 0.01; \*\*\**P* < 0.001.

relationships of the peptide series, we used computational modeling and docking techniques to study the interaction of the peptide series with A $\beta$  fibril, and relate the interactions of their sidechains to their different activities in preventing aggregation (Figs 1 and 2, Supplementary data Table 1s). The purpose of this study was to identify small molecule peptide mimetics with similar ability to inhibit and reverse A $\beta$  misfolding and aggregation, but with better drug-like properties. We identified two sites on the fibril structure where the most active peptides bound preferentially. As  $\beta$ -sheet breakers bind to the fibril at different positions and the fibril may have different conformations, we used the pharmacophores (schematic structures of an ideal small molecule inhibitor) from the 3D-quantitative structure–activity relationship (3D-QSAR; the crossvalidated  $r^2$  ( $q^2$ ) for the  $\beta$ -sheet breakers is only about 0.5) only as approximate guidance for the relative positioning of reactive groups. To obtain more detailed 3D-pharmacophores, we relied on docked conformations of the active peptides with the fibril structure (Fig. 3). These were used to screen the NCI database, a diverse library which includes many drug like molecules, for potential aggregation inhibitors. A small group of compounds were then selected for testing in a medium throughput assay (Table 1), and two compounds were identified as consistently active in preventing and reversing A $\beta$  fibrillogenesis (Fig. 5), measured in three different ways, and blocking A $\beta$  neurotoxicity (Fig. 6). For these initial experiments, we used the smaller NCI database. Now that we have a better idea of what constitutes an active aggregation inhibitor, larger databases such as ZINC (<http://zinc.docking.org>), may be used for future investigations.

The basis for this study was previous work, where we used pharmacophore design and AUTODOCK to find small compounds that bound to the Anthrax edema factor.<sup>36,37</sup> AUTODOCK was quite accurate in finding the conformation and docking position of substrate analogues (i.e., the docked conformation matched the conformation determined by X-ray crystallography).<sup>37</sup> However, docking energies were only approximate indicators of activity.<sup>36,37</sup> Here, we faced a more difficult challenge, as we had several possible structures for the A $\beta$  fibril, and only indirect evidence for where aggregation inhibitors should bind. Moreover, we knew from the peptide data that we could not rely on docking/binding energies to indicate which inhibitors would be most active in inhibiting the aggregation of A $\beta$ . We thus decided to select molecules that resembled the docked conformations of the most active peptides, and then test molecules that had good molecular properties, and similar or higher calculated binding affinities for these sites. A summary of our data indicates that the molecule with the highest calculated binding affinity (first in Table 1) was a very poor inhibitor, and indeed was later used as a negative control. Our two best inhibitors had only slightly better binding affinity than the best  $\beta$ -sheet breaker peptides. This illustrates the complexity of using calculated binding energies to identify inhibitors of the aggregation process, and the need for experimental data to direct the selection process.

One explanation for our results would be that our good inhibitors, such as the peptide LPFFD and BSBM6 and BSBM7, interfere with electrostatic interactions during aggregation<sup>38</sup> or destabilize the A $\beta$ -fibril internal hydrogen bond network, necessary to maintain the  $\beta$ -sheet structure, by forming strong hydrogen bonds with the A $\beta$  subunits. The lowest energy docked conformations of active compounds, such as the peptide LPFFD, and BMBS6 and BMBS7, show hydrogen bonds (red arrows in Figure 7C for BSBM7 and 7D for LPFFD) that would compete with inter-monomer ones. These hydrogen bonds between the ligand and the fibril would be expected to weaken or break the hydrogen bond network stabilizing the sheets, and thereby inhibit or reverse aggregation of A $\beta$ . While C1 has high affinity for the fibril, according to the docking scores, one reason for inactivity could be that the large multi-cyclic

part of C1 (Fig. 5, top right) could also nucleate the formation of even larger aggregates. Continuing with our analysis, inactive compounds such as C1 and the inactive peptide LTicFFD (please see Table S1) form hydrogen bonds with atoms of A $\beta$  that do not form network stabilizing bonds with neighboring monomers (blue arrows in Fig. 7A and B). Thus, we hypothesize, based on docking, that our active compounds interfere with bonds needed to maintain the inter-monomer sheets, while the inactive ones do not. Molecular dynamic simulations for C1, LPFFD, LHFFD, BMBS6 and BMBS7 (manuscript in preparation) show that the active compounds bind more strongly to the fibril than inactive ones. This result agrees with a study by Bernard Reif's group<sup>28</sup> on the interaction of A $\beta$  fibrils with two peptides, a good inhibitor (LPFFD) and a weak one (DPFFL) which showed clearly that DPFFL had a much higher on/off rate (in both Biacore and NMR studies).

These results indicate that molecular docking can be used to discriminate features of compounds that are important for activity, even when the overall docking energies do not directly correlate with activity. Considering the success of the first screening, we plan to redesign the active compounds to further analyze the role of substituents in preventing aggregation. In future work, we will also analyze the calculated H-bond networks of the docked conformation of the compounds that meet our structural criteria, and use this information to select compounds for experimental testing. This approach should lead to the identification of potent and specific  $\beta$ -sheet breaker mimetics to inhibit and reverse A $\beta$  misfolding and oligomerization and thus offer a new avenue for developing drugs for AD treatment.

#### 4. Conclusions

This work's major significance is that the two compounds we identified, that inhibit and reverse A $\beta$  aggregation and neurotoxicity, are possible lead compounds for AD treatment, as they are easy to produce and have low toxicity to cells. Two of the 16 compounds inhibited aggregation at less than equimolar concentration with A $\beta$  in the assay, in the range of 2–3  $\mu$ M. The compounds showed good activity in four different set of experiments, with different methods for measuring aggregates: in preventing aggregation of soluble A $\beta$ , measured by ThT fluorescence or by centrifugation followed by quantitation with ELISA, in disaggregating preformed A $\beta$  fibrils, and in inhibiting the neurotoxic effects of A $\beta$  on cultured neuroblastoma cells. As our least active compound (the C1 control in the assay of Figures 5 and 6) had the most favorable (lowest) docking score, we conclude that we must analyze not just how many bonds a compound is capable of forming with the aggregate, a number summarized broadly in docking scores, but also what effect those bonds will have on destabilizing the inter-subunit contact areas.

The next phase of our work will be to better define the mechanism by which our active compounds inhibit and reverse the aggregation of A $\beta$ . One way will be to test variations on our active compounds that, according to their docked structures, form bonds that should destabilize the aggregates. Additional data on the position of the ligands on the fibril, for example from solid state NMR, would also aid in our search for more active derivatives.

#### 5. Experimental

##### 5.1. Structural model selection for amyloid $\beta$ peptides

The docking targets were fibril structures of A $\beta$ 1–40, prepared in a fashion similar to the methods for inducing aggregation of A $\beta$  used for the experiments below, determined with solid state NMR.<sup>8–11</sup> TEM images and MPL data from STEM images of A $\beta$ 1–

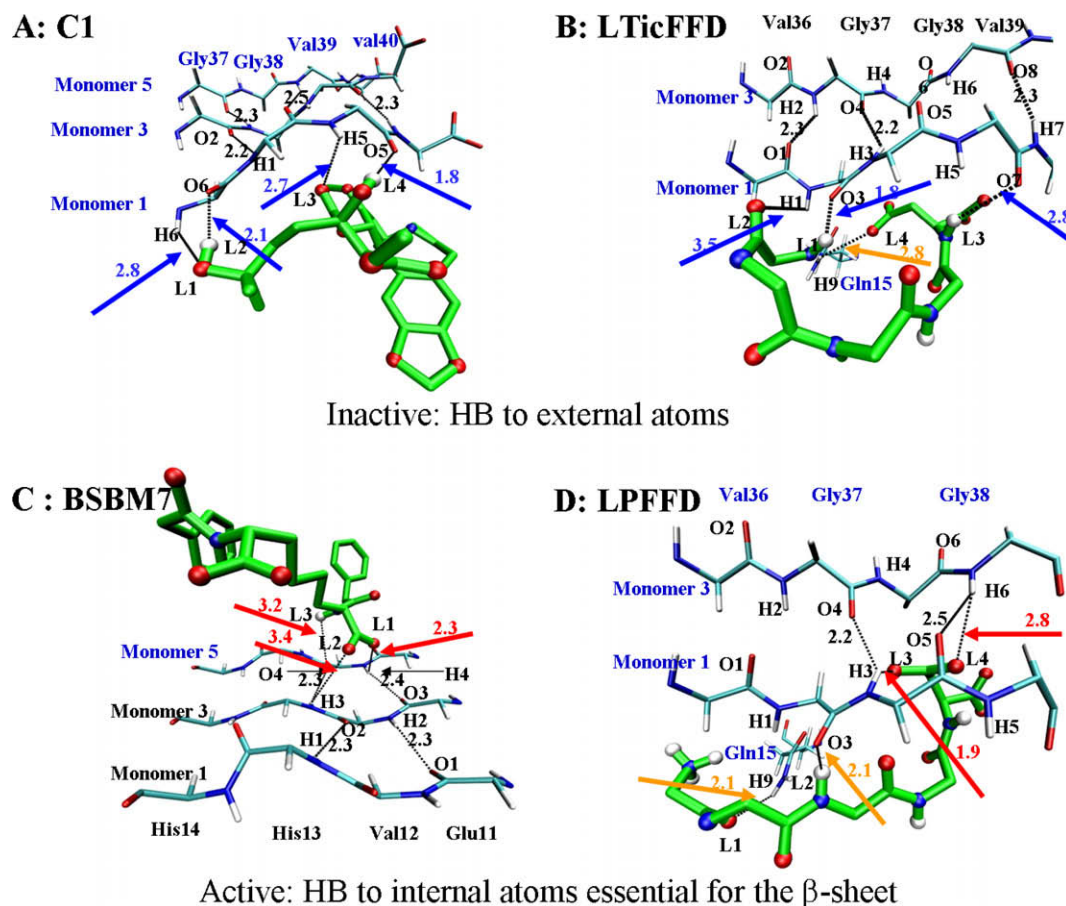


**Figure 7.** Comparison, based on the the best ranked conformations (lowest binding scores) from AUTODOCK, of the type of hydrogen bonds formed between atoms of the bad aggregation inhibitors (A, B) and good ones (C, D) and the fibril. The side chains of the pentapeptides LTicFFD (inactive) and LPFFD (active) are not shown. The hydrogen bonds between ligands and fibril are indicated by red arrows (those that would be expected to break or weaken the  $\beta$  sheet hydrogen bond network of the fibril) and blue arrows (those expected to enhance the stability of the  $\beta$  sheet hydrogen bond network). Yellow arrows indicate those close interactions that should not affect  $\beta$  sheet hydrogen bond network.

42 are very similar to those of agitated A $\beta$ 1–40 fibrils, suggesting that the structure of fibril A $\beta$ 1–42 is very similar to A $\beta$ 1–40.<sup>39</sup> PDB-formatted files for these fibril structures were obtained directly from Dr. Robert Tycko at the NIH (A $\beta$ 40m2\_1.pdb, and A $\beta$ 40p2\_1.pdb, which differ in the orientation of the strands). The structures of A $\beta$ 40m2\_1.pdb and A $\beta$ 40p2\_1.pdb are different in the monomer stacking within the  $\beta$ -sheets.<sup>11</sup> Conformational data were available for residues from Gly9 to Val40; residues 1–8 were highly disordered. The conformation of a (weak)  $\beta$  sheet breaker peptide, DPFFL, bound to fibrillar A $\beta$ 1–40, determined using transferred nuclear Overhauser effect (trNOE) and transferred residual dipolar couplings (trRDC) were used as reference<sup>28</sup>.

## 5.2. Inhibitor peptides for docking

Activity data for a group of peptides related to LPFFD and DPFFL were previously published.<sup>25</sup> These activities are reiterated, together with docking energies for the peptides binding to the fibril, in Supplementary data, Table 1.

## 5.3. Docking and scoring

Selection of the optimal docking site for the active peptide series on the NMR fibril structures A $\beta$ 40m2\_1.pdb and A $\beta$ 40p2\_1.pdb was done with AUTODOCK <http://www.scripps.edu/mb/olson/doc/autodock><sup>40,41</sup> (version 3.0.5), using the ‘Lamarckian’ genetic algorithm (LGA). To allow the ligands to rotate freely over the whole

structure to determine the approximate region of preferred docking to the fibril, the grid box size was set initially to 120  $\times$  110  $\times$  90 points with grid spacing of 0.60 Å and centered on the center of the A $\beta$  fibril. The optimal site on the fibril for each peptide was refined by repeating the docking with a smaller grid box (either 60  $\times$  60  $\times$  60 or 80  $\times$  80  $\times$  80 points with grid spacing of 0.375 Å). During docking, the A $\beta$  fibril was kept rigid and 200 conformations of the flexible ligand peptide (LPFFD and related) were searched and docked. Other parameters were default, except the population size (100). AUTODOCK docking energy, which estimates the intermolecular potential energy between the ligand and A $\beta$  and the torsional free energy of ligand, was minimized.

## 5.4. 3D-Pharmacophore design

Our previous work showed that AUTODOCK is quite accurate in positioning molecules on a given target and determining lowest energy conformations.<sup>37</sup> Pharmacophores representing an optimal configuration of the active groups of the active peptides were derived, with distance constraints obtained from the lowest energy docking conformations of LPFFD on the two A $\beta$  models A $\beta$ 40m2\_1.pdb and A $\beta$ 40p2\_10.pdb. The pharmacophore features, such as HBA (including negatively charged groups), HBD (including positively charged groups), and hydrophobic (HP), were defined manually based on the interactions of LPFFD with the A $\beta$  fibril. A hydrogen bond interaction was defined if any atom of LPFFD was within 2.8 Å of any atom of the fibril. HP was defined if the hydro-



phobic groups or atoms of the ligands were close ( $<4.0 \text{ \AA}$ ) to the hydrophobic groups or atoms of A $\beta$ .

### 5.5. Database screening and molecular docking

The resulting 3D-pharmacophores were used for 3D-database screening with the UNITY program (Tripos, Inc.) in SYBYL7.1. The NCI-2000 database, integrated in SYBYL, with about 250,000 compounds stored as 3D structures converted from their 2D forms by Concord, was screened for compounds matching the pharmacophores, using tolerance for HBA and HBD features of  $0.3 \text{ \AA}$  and for HP of  $0.8 \text{ \AA}$ .

Selected compounds were docked to fibril sites 1 and 2 of the two A $\beta$  models A $\beta$ 40m2\_1.pdb and A $\beta$ 40p2\_10.pdb with AUTODOCK, using the methods described above, and ranked according to their docking scores. Compounds with cLog P  $<5$  and molecular weight  $<500$  were considered if their binding energies were lower than the binding energy of LPFFD. Highest priority was given to compounds selected several times in the UNITY searches with the different pharmacophores.

### 5.6. Preparation of A $\beta$ peptide and compounds for the aggregation assay

A $\beta$ 1–42 was synthesized using solid phase chemistry by the protein core at Yale University (W.M. Keck Facility, University of Yale). 0.3 mg of lyophilized powder was dissolved in 200  $\mu\text{l}$  of hexafluoro-2-propanol (Sigma–Aldrich) for 10–20 min at room temperature. Soluble A $\beta$  was made by drying the HFIP and adding H $_2\text{O}$  in a siliconized Eppendorf tube to obtain a final peptide concentration of 60  $\mu\text{M}$ . For the experiments, A $\beta$  was diluted to 3.3  $\mu\text{M}$  in 0.1 mM Tris in the absence and presence of selected small molecules at a one to one molar ratio. Compounds were obtained in powder form from the stock collection of the Developmental Therapeutics Program (DTP), NCI, Bethesda, MD (<http://dtp.nci.nih.gov>) and dissolved in DMSO to 0.4 mM for storage at  $-20^\circ\text{C}$ . They were diluted 100X in Hepes, pH 7.0, before adding to the assay. The same amount of DMSO was added to the controls.

### 5.7. Assays for aggregation inhibition

The compounds were screened first with a medium throughput in vitro fluorometric assay based on the fluorescence emission of thioflavin T (ThT) when bound to amyloid fibrils.<sup>42</sup> Soluble A $\beta$  peptide at a concentration of 3.3  $\mu\text{M}$  in 0.1 M Tris buffer was incubated alone or with the indicated concentrations of the compounds for 24 h at  $37^\circ\text{C}$ . Aliquots (20  $\mu\text{l}$ ) of samples were incubated 15 min at room temperature in 50 mM glycine, pH 9.2 and 2  $\mu\text{M}$  ThT. Fluorescence was measured at excitation wavelength of 435 nm with emission at 485 nm. Compounds **1**, **6** and **7** (3.3  $\mu\text{M}$ ) were further tested for their ability to disassemble pre-formed fibrillar A $\beta$  after incubation for 24 h. As control soluble (non-fibrillar) A $\beta$  and fibrils incubated alone were included. The quantity of fibrils was measured by ThT fluorescence. To rule out that the compounds interfere with ThT fluorescence, the effect of the compounds alone on the assay was measured.

A $\beta$  aggregates were also assayed by sedimentation. After incubation with or without compounds, samples were centrifuged at 16,000g for 10 min at  $4^\circ\text{C}$ . Soluble peptide was measured in the supernatant by ELISA using the 4G8 anti-A $\beta$  monoclonal antibody.

### 5.8. Neuronal toxicity assay

Compounds **1**, **6** and **7** (3.3  $\mu\text{M}$ ) were incubated with soluble A $\beta$  (3.3  $\mu\text{M}$ ) for 48 h. Controls were soluble A $\beta$  incubated at the same concentration either with addition of the inactive compound **1** or

the same amount of DMSO (the final concentration of DMSO in all assays was  $<0.1\%$ ). Aliquots of samples (10  $\mu\text{l}$ ) were added to 80% confluent mouse neuroblastoma cells N2a, incubated 24 h in a 96 well plate at  $37^\circ\text{C}$  in a humidified, 5% CO $_2$  atmosphere. Cell survival was assessed by the MTS assay (Promega). The combined MTS/PMS solution (20  $\mu\text{l}$ ) was added to the culture medium and the cells were incubated 1–4 h at  $37^\circ\text{C}$  in a humidified, 5% CO $_2$  atmosphere. Absorbance was read at 490 nm.

### Acknowledgments

We thank Dr. Rakez Kaye (Neurology, UTMB) for his advice and assistance with the assays. This work was supported by a Pilot Award from the George and Cynthia Mitchell Center for Neurodegenerative Diseases to Catherine Schein, grants from the NIH (AG028821) and the Mitchell Foundation to Claudio Soto. The infrastructure of the Sealy Center for Structural Biology and Molecular Biophysics, and of the Sealy Center for Vaccine Design, were also used. Compounds used in this study were obtained from the stock collection of the Developmental Therapeutics Program (DTP), NCI, Bethesda, MD (<http://dtp.nci.nih.gov>).

### Supplementary data

Supplementary data associated with this article can be found, in the online version, at doi:10.1016/j.bmc.2009.05.047.

### References and notes

- Hendrie, H. C. *Am. J. Geriatr. Psychiatry* **1998**, 6, S3.
- Alzheimer, A.; Stelzmann, R. A.; Schnitzlein, H. N.; Murtagh, F. R. *Clin. Anat.* **1995**, 8, 429.
- Thal, D. R.; Rub, U.; Orantes, M.; Braak, H. *Neurology* **2002**, 58, 1791.
- Braak, H.; Braak, E. *Neurobiol. Aging* **1995**, 16, 271.
- Selkoe, D. J. *Ann. N.Y. Acad. Sci.* **2000**, 924, 17.
- Cohen, A. S.; Jones, L. A. *Curr. Opin. Rheumatol.* **1991**, 3, 125.
- Soto, C.; Branes, M. C.; Alvarez, J.; Inestrosa, N. C. *J. Neurochem.* **1994**, 63, 1191.
- Petkova, A. T.; Buntkowsky, G.; Dyda, F.; Leapman, R. D.; Yau, W. M.; Tycko, R. *J. Mol. Biol.* **2004**, 335, 247.
- Tycko, R. *Curr. Opin. Chem. Biol.* **2000**, 4, 500.
- Tycko, R. *Methods Enzymol.* **2006**, 413, 103.
- Tycko, R. *Q. Rev. Biophys.* **2006**, 39, 1.
- Kheterpal, I.; Chen, M.; Cook, K. D.; Wetzel, R. J. *Mol. Biol.* **2006**, 361, 785.
- Kheterpal, I.; Wetzel, R. *Acc. Chem. Res.* **2006**, 39, 584.
- Luhers, T.; Ritter, C.; Adrian, M.; Riek-Loher, D.; Bohrmann, B.; Döbeli, H.; Schubert, D.; Riek, R. *Proc. Natl. Acad. Sci. U.S.A.* **2005**, 102, 17342.
- Petkova, A. T.; Yau, W. M.; Tycko, R. *Biochemistry* **2006**, 45, 498.
- Williams, A. D.; Shivaprasad, S.; Wetzel, R. J. *Mol. Biol.* **2006**, 357, 1283.
- Hilbich, C.; Kisters-Woike, B.; Reed, J.; Masters, C. L.; Beyreuther, K. *J. Mol. Biol.* **1992**, 228, 460.
- Jarrett, J. T.; Berger, E. P.; Lansbury, P. T. *J. Ann. N.Y. Acad. Sci.* **1993**, 695, 144.
- Soto, C.; Castano, E. M.; Frangione, B.; Inestrosa, N. C. *J. Biol. Chem.* **1995**, 270, 3063.
- Wood, S. J.; Wetzel, R.; Martin, J. D.; Hurler, M. R. *Biochemistry* **1995**, 34, 724.
- Shivaprasad, S.; Wetzel, R. J. *Biol. Chem.* **2006**, 281, 993.
- Soto, C.; Kindy, M. S.; Baumann, M.; Frangione, B. *Biochem. Biophys. Res. Commun.* **1996**, 226, 672.
- Permanne, B.; Adessi, C.; Saborio, G. P.; Fraga, S.; Frossard, M. J.; Van Dorpe, J.; Dewachter, I.; Banks, W. A.; Van Leuven, F.; Soto, C. *FASEB J.* **2002**, 16, 860.
- Soto, C.; Sigurdsson, E. M.; Morelli, L.; Kumar, R. A.; Castaño, E. M.; Frangione, B. *Nat. Med.* **1998**, 4, 822.
- Adessi, C.; Frossard, M. J.; Boissard, C.; Fraga, S.; Bieler, S.; Ruckle, T.; Vilbois, F.; Robinson, S. M.; Mutter, M.; Banks, W. A.; Soto, C. *J. Biol. Chem.* **2003**, 278, 13905.
- Chacón, M. A.; Barria, M. I.; Soto, C.; Inestrosa, N. C. *Mol. Psychiatry* **2004**, 9, 953.
- Milne, G. W.; Nicklaus, M. C.; Driscoll, J. S.; Wang, S.; Zaharevitz, D. J. *Chem. Inf. Comput. Sci.* **1994**, 34, 1219.
- Chen, Z.; Krause, G.; Reif, B. *J. Mol. Biol.* **2005**, 354, 760.
- Etienne, M. A.; Edwin, N. J.; Aucoin, J. P.; Russo, P. S.; McCarley, R. L.; Hammer, R. P. *Methods Mol. Biol.* **2007**, 386, 203.
- Teplow, D. B. *Biochemistry* **1998**, 37, 121.
- Cohen, F. E.; Kelly, J. W. *Nature* **2003**, 426, 905.
- De Lorenzi, E.; Giorgetti, S.; Grossi, S.; Merlini, G.; Caccialanza, G.; Bellotti, V. *Curr. Med. Chem.* **2004**, 11, 1065.
- Estrada, L. D.; Soto, C. *Curr. Top. Med. Chem.* **2007**, 7, 115.
- LeVine, H. *Curr. Med. Chem.* **2002**, 9, 1121.



35. Mason, J. M.; Kokkoni, N.; Stott, K.; Doig, A. J. *Curr. Opin. Struct. Biol.* **2003**, *13*, 526.
36. Chen, D.; Misra, M.; Sower, L.; Peterson, J. W.; Kellogg, G. E.; Schein, C. H. *Bioorg. Med. Chem.* **2008**, *16*, 7225.
37. Chen, D.; Menche, G.; Power, T. D.; Sower, L.; Peterson, J. W.; Schein, C. H. *Proteins-Struct. Funct. Bioinform.* **2007**, *67*, 593.
38. Yun, S.; Urbanc, B.; Cruz, L.; Bitan, G.; Teplow, D. B.; Stanley, H. E. *Biophys. J.* **2007**, *92*, 4064.
39. Antzutkin, O. N.; Leapman, R. D.; Balbach, J. J.; Tycko, R. *Biochemistry* **2002**, *41*, 15436.
40. Morris, G. M.; Goodsell, D. S.; Halliday, R. S.; Huey, R.; Hart, W. E.; Belew, R. K.; Olson, A. J. *J. Comput. Chem.* **1998**, *19*, 1639.
41. Morris, G. M.; Goodsell, D. S.; Huey, R.; Olson, A. J. *J. Comput. Aided Mol. Des.* **1996**, *10*, 293.
42. LeVine, H. *Protein Sci.* **1993**, *2*, 404.